Computational Biology and Chemistry 105 (2023) 107907

Contents lists available at ScienceDirect

Computational Biology and Chemistry

journal homepage: www.elsevier.com/locate/cbac

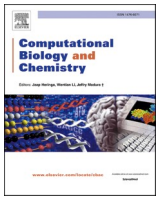

Antihyperlipidemic mechanisms of a formula containing *Curcuma xanthorrhiza, Sechium edule,* and *Syzigium polyanthum*: In silico and in vitro studies

Frangky Sangande [a,*], Kurnia Agustini [a], Krisyanti Budipramana [b]

[a] *Research Center for Pharmaceutical Ingredients and Traditional Medicine, National Research and Innovation Agency (BRIN), Cibinong Science Center, Bogor 16915, Indonesia*

[b] *Department of Pharmaceutical Biology, Faculty of Pharmacy, University of Surabaya, Surabaya 60293, Indonesia*

ARTICLE INFO

Keywords:
Extract combination
Antihyperlipidemic
Network pharmacology
Consensus docking
HMGCR

ABSTRACT

Herbal medicines are multi-component and can exhibit synergistic effects in the treatment of diseases. *Sechium edule, Syzigium polyanthum*, and *Curcuma xanthorrhiza* have been used in traditional medicine to reduce serum lipid levels. However, the molecular mechanism was not described clearly, especially as a mixture. Thus, we performed a network pharmacology study combined with molecular docking to find a rational explanation regarding the molecular mechanisms of this antihyperlipidemic formula. According to the network pharmacology study, we predicted that this extract mixture would act as an antihyperlipidemic agent by modulating several pathways including insulin resistance, endocrine resistance, and AMP-activated protein kinase (AMPK) signaling pathway. Based on the topology parameters, we identified 6 significant targets that play an important role in reducing lipid serum levels: HMG-CoA reductase (HMGCR), peroxisome proliferator-activated receptor alpha (PPARA), RAC-alpha serine/threonine-protein kinase (AKT1), epidermal growth factor receptor (EGFR), matrix metalloproteinase-9 (MMP9), and tumor necrosis factor-alpha (TNF). Meanwhile, 8 compounds: β-sitosterol, bisdesmethoxycurcumin, cucurbitacin D, cucurbitacin E, myricetin, phloretin, quercitrin, and rutin were the compounds with a high degree, indicating that these compounds have a multitarget effect. Our consensus docking study revealed that HMGCR was the only protein targeted by all potential compounds, and rutin was the compound with the best consensus docking score for almost all targets. The in vitro study revealed that the extract combination could inhibit HMGCR with an IC_{50} value of 74.26 μg/mL, indicating that HMGCR inhibition is one of its antihyperlipidemic mechanisms.

1. Introduction

Hyperlipidemia is a chronic metabolic disease, strongly related to several high-incidence cardiovascular diseases, including diabetes, coronary heart disease, atherosclerosis, and hypertension (Nelson, 2013). Hyperlipidemia is characterized by an imbalance of lipid serum levels including increased total cholesterol, low-density lipoprotein (LDL), triglycerides (TG), and decreased high-density lipoprotein (HDL) (Su et al., 2021). In addition, herbal products could be complementary or alternative treatments for hyperlipidemia to conventional medicine such as statins, fibrates, and bile acid sequestrants (Hasani-Ranjbar et al., 2012).

In traditional medicine, herbal products may contain a single herb or multiple herbs. However, numerous studies have shown that in some cases, the combination of herbs provides efficacies over a single herb in equivalent doses (Che et al., 2013; Zhou et al., 2016). As a single herb, roots of *Rehmannia glutinosa* or *Astragalus membranaceus* did not show a wound-healing effect in a foot ulcer animal model. However, their combination in a ratio of 2:1 resulted in a significant effect (Lau et al., 2012). Another study showed that the addition of *Magnolia officinalis* and *Citrus aurantium* can induce higher bioavailability of genoposide in rats, suggesting that herb-herb interaction could influence the bioavailability of the active ingredient (Sun et al., 2012). Meanwhile, an in vivo study demonstrated ginger can detoxicate the toxicity of Pinellia rhizoma by reducing the prostaglandin E2 level induced by Pinellia rhizoma (Wu et al., 1998). These studies indicated that herbs

* Corresponding author.
E-mail address: fran015@brin.go.id (F. Sangande).

https://doi.org/10.1016/j.compbiolchem.2023.107907
Received 2 May 2023; Received in revised form 14 June 2023; Accepted 17 June 2023
Available online 20 June 2023

combination may improve the pharmacokinetic and pharmacodynamic profiles, as well as the toxicity profile, of their formula.

Indonesia with its high biodiversity is promising to develop natural products as a source of drugs (Arifah et al., 2022). In the case of hyperlipidemia treatment, numerous medicinal plants have been used traditionally. Among them, *Curcuma xanthorrhiza* (Yasni et al., 1993), *Sechium edule* (Mohammed et al., 2022), and *Syzigium polyanthum* (Hartanti et al., 2019) have been reported to reduce serum lipid levels. In a previous study, extract combination of *Sechium edule* fruit, *Syzigium polyanthum* leaf, and *Curcuma xanthorrhiza* rhizome showed a good effect in reducing cholesterol total and triglyceride levels on male rats induced by high cholesterol diet (Agustini et al., 2006). However, its mechanism has not been elucidated yet. This is one of the problems in natural product drug discovery based on phenotypic assays (Atanasov et al., 2021), especially since the natural products are still in extract material. The complexity of multi-compound materials presents a challenge in the molecular target determination of extract formula obtained experimentally.

Currently, the main methods for determining the molecular target have been tedious and time-consuming such as genomic and proteomic approaches (Ou-Yang et al., 2012). Fortunately, in the big data era, network pharmacology is a useful approach because it can guide a researcher in studying the molecular mechanism, and selecting the potential compounds as well as the targets that play an important role in the treatment of diseases (Noor et al., 2022). Furthermore, molecular docking simulations have been used to validate the prediction of network pharmacology based on the interaction capability of potential compounds against the corresponding target (Li et al., 2022; Liu et al., 2022; Zhang et al., 2021).

2. Material and methods

2.1. Collection of active compounds and their targets prediction

The constituents information of *C. xanthorrhiza* rhizome, *S. edule* fruit, and *S. polyanthum* leaf was obtained from the literature (Atanasov et al., 2021; Iñiguez-Luna et al., 2021; Ismail et al., 2019; Riviello-Flores et al., 2018) and Dr. Duke's Phytochemical and Ethnobotanical Databases. This database provides active compounds in every part of the plant thereby we can select active compounds from the appropriate part. Their potential targets were predicted using SwissTargetPrediction based on chemical similarity (http://www.swisstargetprediction.ch/). Targets with a probability ≥ 0.1 were selected.

2.2. Collection of potential targets for hyperlipidemia

Due to the different sources, every database may provide different results regarding the disease-related target. Therefore, in the current study, GeneCards (https://www.genecards.org/) and CTD databases (http://ctdbase.org/) were used for retrieving as many hyperlipidemia-related targets as possible by using "hyperlipidemia" as the keyword. The targets obtained from the two databases were combined, and the duplicate targets were deleted. Afterward, this merged result was overlaid with the potential targets of the active compounds in step 2.1 using the Venny 2.1 tool (https://bioinfogp.cnb.csic.es/tools/venny/index.html). The intersection targets were selected as the targets of the active compounds for the treatment of hyperlipidemia.

2.3. GO and KEGG analysis

The intersection targets from step 2.2 was imported to ShyniGO 0.77 (http://bioinformatics.sdstate.edu/go/), a graphical tool integrated with STRING and Ensembl databases, to analyze and visualize the Gene Ontology (GO) biological process and Kyoto Encyclopedia of Genes and Genomes (KEGG) enrichment. In this web tool, the p-value was set to 0.05. Twenty items with the highest enrichment were recommended and visualized on the bar graph automatically. For the KEGG result, we selected the pathways manually based on relevance to hyperlipidemia.

Table 1
Center coordinates in the Vina protocol.

Target	Center coordinates		
	x	y	z
TNF	-15.168	-2.292	-26.225
AKT1	-20.286	3.748	11.736
EGFR	21.697	0.303	52.093
MMP9	2.656	7.583	21.734
PPARA	15.324	39.880	27.766
HMGCR	19.364	7.605	15.470

2.4. Construction of the compound-target (CT) network

Compounds without targets included in the intersection target list were removed. We constructed the network of remaining active compounds and their corresponding target by importing the data into Cytoscape and the mean value of the degree at every compound was calculated. Compounds with a degree value greater than the mean value (> 4.9) were considered potential compounds for further analysis in molecular docking simulation.

2.5. Construction of protein-protein interaction (PPI) network

The STRING database (https://string-db.org/) on Homo sapiens with default parameters was used to construct the PPI network of the intersection targets in step 2.2. For further analysis, the PPI network gained from STRING was imported into Cytoscape 3.9.3 to calculate six topology parameters of the intersection targets including degree centrality (DC), betweenness centrality (BC), closeness centrality (CC), eigenvector centrality (EC), network centrality (NC), and local average connectivity (LAC) using the CytoNCA plugin. The mean values of every topology parameter were used as the cutoff, and targets with a value of six parameters greater than or equal to the mean value (DC $\geq$ 8.830, BC $\geq$ 42.976, CC $\geq$ 0.509, EC $\geq$ 0.127, NC $\geq$ 6.728, LAC $\geq$ 4.265) and also having degree ≥ 2 based on the compound-target network (step 2.4) were selected as potential targets.

2.6. Molecular docking simulation

For molecular docking simulation, the 3D structure of the selected compounds was downloaded from PubChem as sdf and converted to pdb using Discovery Studio. While the crystal structures of TNF (PDB:7JRA), AKT1 (PDB:4GV1), EGFR (PDB:1M17), MMP9 (PDB:4WZV), PPARA (PDB:2P54), HMGCR (PDB:1HWK) were downloaded from RCSB. Docking simulations were performed using two docking tools, Vina and DOCK6.

In Vina, the targets and ligands were prepared using AutoDock Tool 1.5.6. At this stage, the polar hydrogen atoms, Kollman charges for targets, and Gasteiger charges for ligands were added. For all docking calculations, a grid box centered on the native ligand with a dimension of 22 $\times$ 22 x 22 Å at 1 Å spacing was used. The center coordinates x, y, and z of TNF, AKT1, EGFR, MMP9, PPARA, and HMGCR are presented in Table 1.

In DOCK6, the targets and ligands were prepared using USCF Chimera. At this stage, hydrogen atoms will be added. AMI-BBC method was used for adding the charges. The probe radius in the DMS was set to 1.4 Å to generate the molecular surface. The active site was defined in 8 Å radius about the native ligand and 5 Å extra margin in all six directions was applied to form the box around the active site. In both docking tools, the number of conformations per ligand was set to 10. Consensus docking was implemented by combining the docking results of DOCK6 and Vina as described in a previous study (Gimeno et al., 2020). Here,

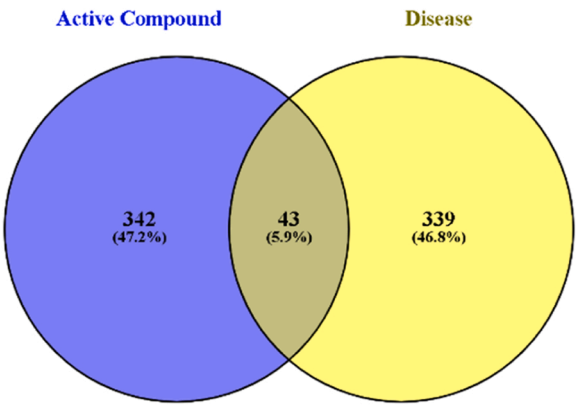

Fig. 1. Venn diagram of overlapping between active compound-related targets and disease-related targets.

virtual hits were defined as compounds showing equivalent conformation (docking pose) in both docking tools, DOCK6 and Vina. The consensus score was calculated by averaging the scores of the two equivalent docking poses.

2.7. In vitro study

Extracts of *C. xanthorrhiza* rhizome, *S. edule* fruit, and *S. polyanthum* leaf were obtained by maceration (1:10) for three days using ethanol at 96 %, 50 %, and 70 % for *C. xanthorrhiza* rhizome, *S. edule* fruit, and *S. polyanthum* leaf, respectively. The extracts were then evaporated using a rotary evaporator to obtain concentrated extracts. The activities of *C. xanthorrhiza* rhizome, *S. edule* fruit, and *S. polyanthum* leaf extracts were tested on HMGCR. The HMGCR assay kit was purchased from Sigma-Aldrich. The enzyme, substrate, and buffer solutions were prepared according to the manufacturer's instructions using a 96-well plate format.

We performed an enzymatic assay for the percentage of inhibition calculation of each extract and the combination of *S. edule, S. polyanthum, C. xanthorrhiza* (5:1:5) at a single concentration. Test solution (40,000 μg/mL) of each extract and the combination was prepared by dissolving 40 mg extracts in 100 μL of 96 % ethanol before diluting it to 1 mL using ultrapure water. 1 μL of this test solution was used in the enzymatic reaction at a final volume of 200 μL. Thus, the final concentration of the test solution was 200 μg/mL. Meanwhile, IC_{50} determination was only carried out on the extract combination. Stock solution (80,000 μg/mL) was prepared by dissolving 80 mg of the extract combination (5:1:5) in 100 μL of 96 % ethanol before diluting it to 1 mL using ultrapure water. Afterward, 5 points 1:2 serial dilution was

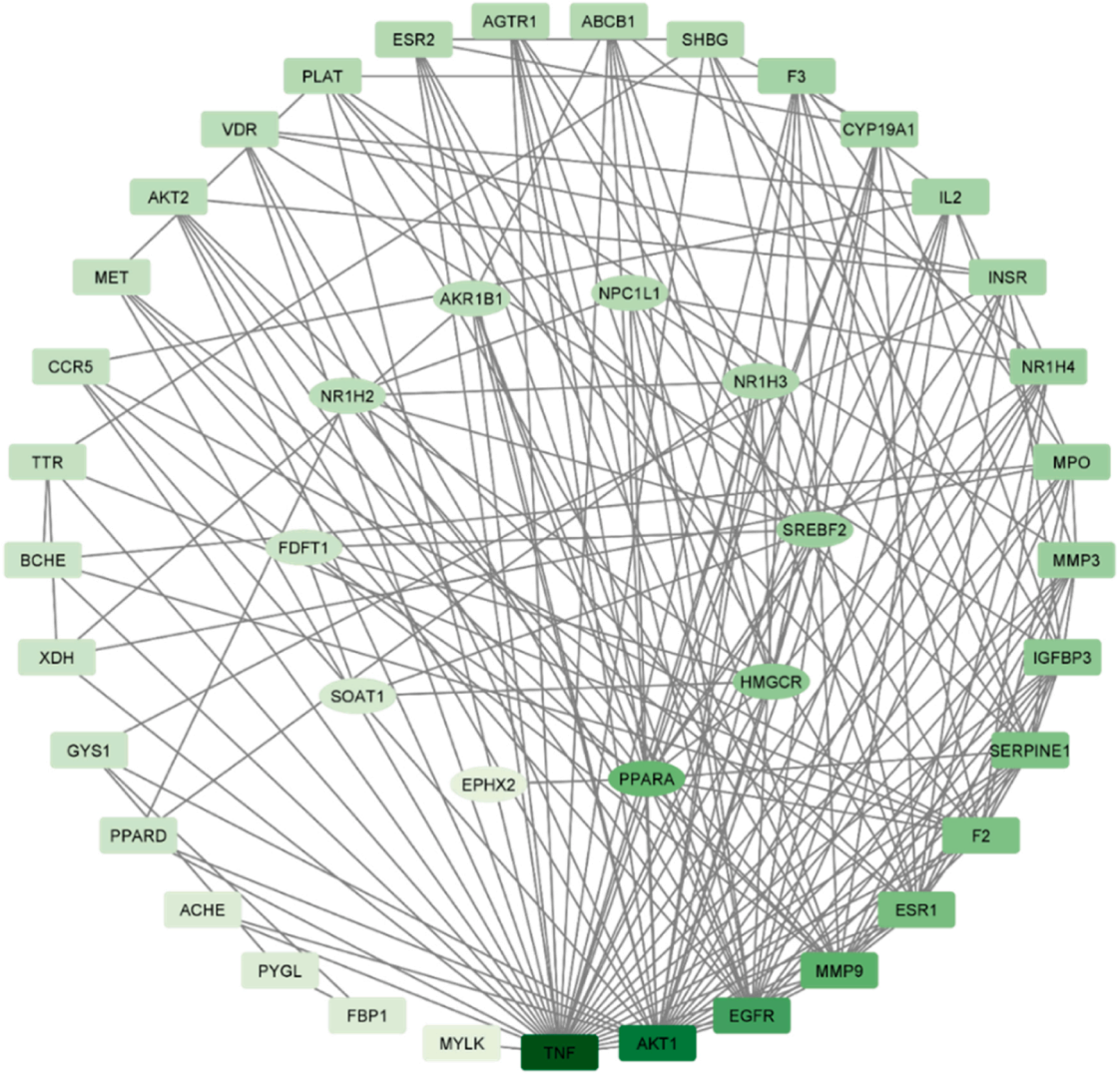

Fig. 2. Protein-protein interaction network of 43 potential targets.

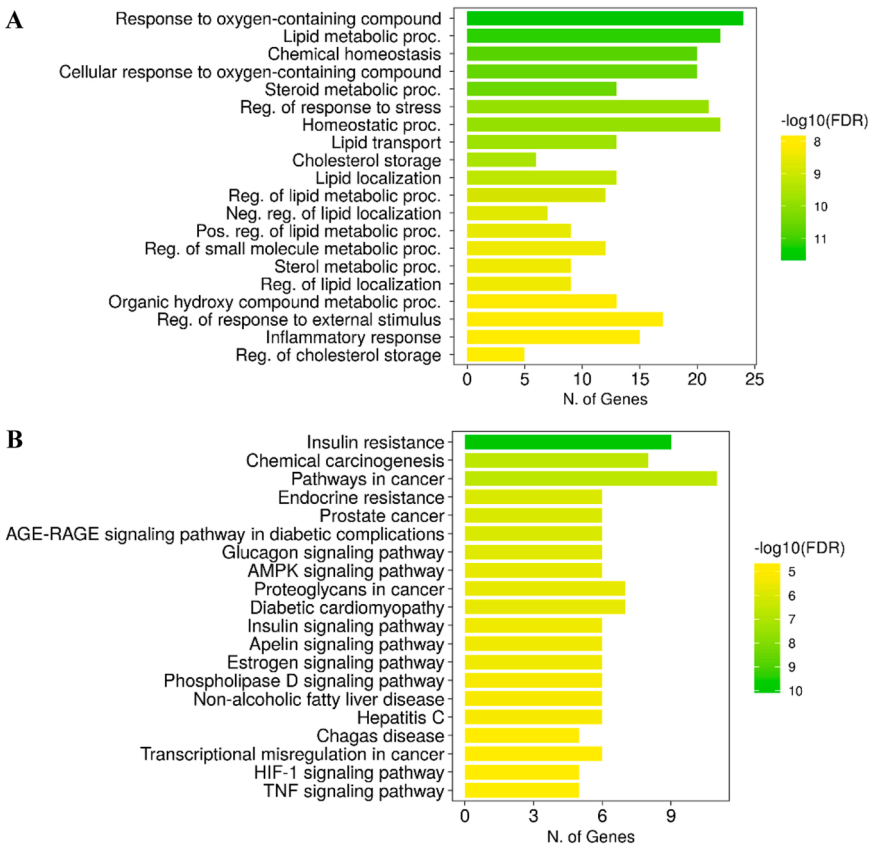

Fig. 3. Biological process (A), and KEGG pathways enrichment (B).

prepared to produce 5000–80,000 μg/mL test solution. Similar to the single concentration test, 1 μL of these test solutions was used in 200 μL of the enzymatic reaction to give the final concentration of 25–400 μg/mL.

The enzymatic reaction with two replicates was performed in a 96-well plate. Every well consists of 1 μL of test solution, 181 μL of 1x assay buffer, 4 μL of NADPH, 12 μL of HMG-CoA, and 2 μL of HMGCR. For the control (HMGCR without inhibitor or test solution) well, the same composition was used, but the volume 1x assay buffer was 182 μL. The absorbance was read at λ 340 nm every 20 s for 10 min at a temperature of 37 °C. The percentage of inhibition was calculated using the following formula and the IC_{50} was calculated using GraphPad Prism 8.0.2.

$$\%Inhibition = \frac{\frac{\Delta A}{\Delta T}\ Control - \frac{\Delta A}{\Delta T}\ Test\ \ solution}{\frac{\Delta A}{\Delta T}\ Control} \times 100$$

3. Results

3.1. Active compounds collection and their potential targets

After searching literature and databases, we successfully collected 21 active compounds of this extract combination that have potential targets with probability ≥ 0.1 % based on SwissTargetPrediction. These compounds were known to have 385 targets.

3.2. Screening of potential targets for hyperlipidemia

From the 385 targets listed above, the objective for hyperlipidemia still needs to be determined. For this purpose, we collected 382 hyperlipidemia-related targets after merging the results from the GeneCards and CTD databases. When the active compound-related targets database was mapped to the disease-related targets database using Venny tools, we found 43 potential targets were in the intersection area (Fig. 1).

3.3. PPI, GO, and KEGG analysis

For further investigation, we built the protein-protein interaction (PPI) of the 43 possible targets and obtained 190 edges. The edges represent the interaction between targets, while the nodes represent the 43 targets. A darker green color indicated a greater degree value for a node (Fig. 2).

According to ShyniGO, the top 20 GO biological processes were all strongly related to the storage and metabolic process of lipid derivate (Fig. 3A), with response to oxygen-containing compounds ranking first. Ten of them, as depicted as elips nodes in Fig. 2 were involved in the lipid metabolic process (GO:0006629): AKR1B1, EPHX2, NR1H3, PPARA, FDFT1, HMGCR, NPC1L1, NR1H2, SOAT1, SREBF2. Meanwhile, based on the top 10 pathways rank, KEGG results suggested that this formula might work as an antihyperlipidemic through the regulation of insulin resistance, endocrine resistance, and the AMPK signaling pathway, in addition to cancer-related pathways (Fig. 3B).

3.4. Identification of potential compounds and potential targets

Based on the active compound-target network, we identified 9 potential compounds with degree values above the average: alnustone, β-sitosterol, bisdesmethoxycurcumin, cucurbitacin D, cucurbitacin E, myricetin, phloretin, quercitrin, and rutin. However, alnustone was excluded because it can not be docked successfully using DOCK6 in the current protocol. Interestingly, these potential compounds represented three herbs, thus supporting why the combination of the three herbs was used as the antihyperlipidemic formula. Bisdesmethoxycurcumin and alnustone are from *C. xanthorrhiza* rhizome; β-sitosterol and quercitrin

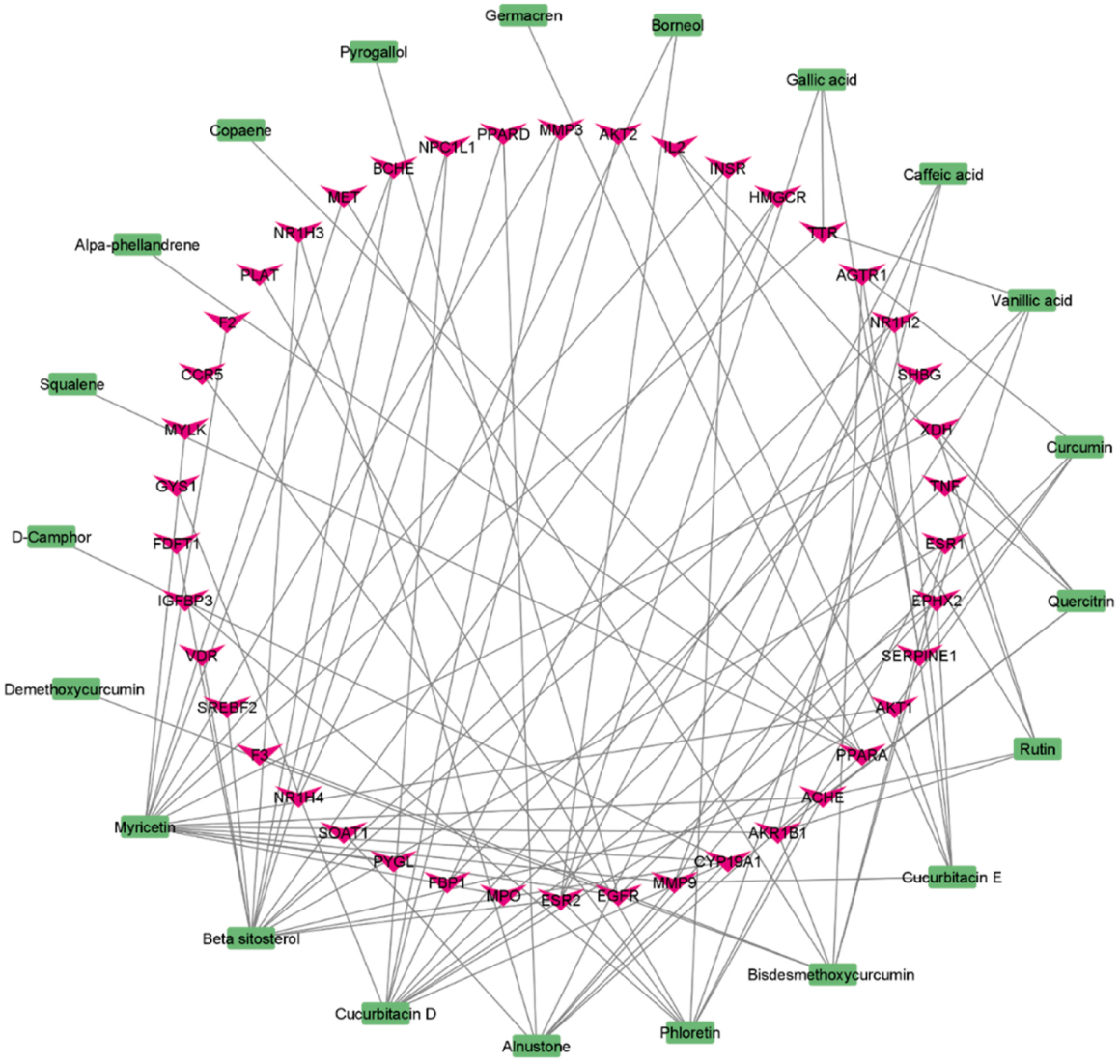

Fig. 4. Compound-target (CT) network. Green nodes represent the active compounds, and magenta nodes represent the targets.

Table 2
Topology parameters of the targets based on the PPI network and CT network.

Target	PPI network						CT network
	DC	EC	LAC	BC	CC	NC	DC
TNF	33	0.365	7.576	514.923	0.792	29.302	3
AKT1	28	0.339	7.928	401.406	0.750	23.685	4
EGFR	21	0.283	7.619	97.983	0.636	16.394	5
MMP9	18	0.262	8.222	49.519	0.609	15.113	5
PPARA	17	0.213	5.647	192.599	0.609	10.233	5
HMGCR	12	0.136	5.167	80.552	0.567	8.921	2
Cutoff	8.830	0.127	4.265	42.976	0.509	6.728	2

are from *S. polyanthum* leaf; cucurbitacin D, cucurbitacin E, myricetin, phloretin, and rutin are from *S. edule* fruit.

On the other hand, according to the six topology parameters analysis on the PPI network (Fig. 2) and targets degree on the CT network (Fig. 4), we identified 6 targets with values greater than or equal to the cutoff (Table 2).

3.5. Molecular docking

Before the simulation, the docking protocols against 6 targets using DOCK6 and Vina were validated. Table 3 showed that all docking protocols can reproduce the crystallography pose of the native ligand with a favorable rmsd value (< 2 Å). Furthermore, docking simulation using the consensus method of 8 compounds against the 6 targets revealed that HMGCR is the only target that can produce a duplet binding pose for all compounds. The docking scores of DOCK6, Vina, and the consensus method were presented in Tables 4–6, respectively. Compounds without a score in certain targets, indicating that they had no duplet conformation.

Based on Table 6, rutin showed the best consensus score against

Table 3
Superimposition of the redocking pose native ligands and their crystallography pose.

Target	DOCK6	Vina
TNF	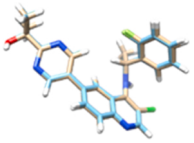	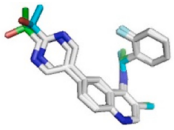
AKT1	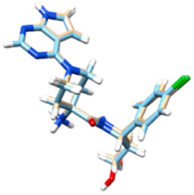	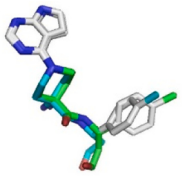
EGFR	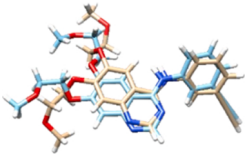	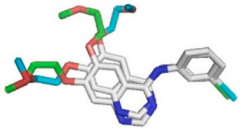
MMP9	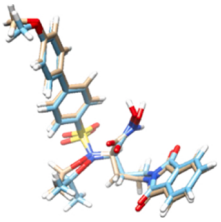	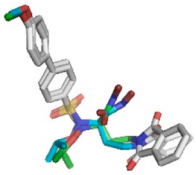
PPARA	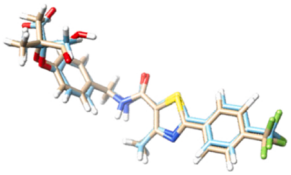	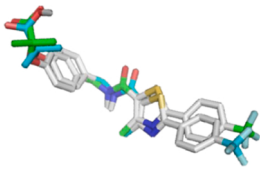
HMGCR	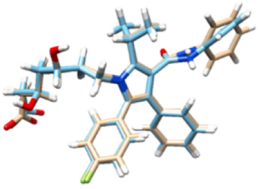	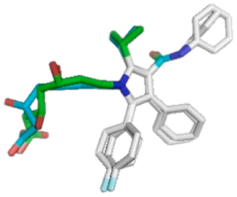

Table 4
DOCK6 score of potential compounds against potential targets.

Compound	DOCK6 score					
	TNF	AKT1	EGFR	MMP9	PPARA	HMGCR
β-sitosterol	–	-59.7	–	–	–	-55.3
Bisdesmethoxycurcumin	-64.8	-60.6	-56.9	–	-60.6	-52.2
Cucurbitacin D	–	-66.1	-58.7	–	–	-61.5
Cucurbitacin E	–	-67.5	–	–	–	-64.8
Myricetin	-52.6	-58.9	-59.0	-57.9	-51.8	-51.5
Phloretin	-50.6	–	-49.3	–	-48.6	-50.7
Quercitrin	–	–	-58.1	-64.9	-50.8	-64.9
Rutin	–	-88.9	-48.9	-78.4	-82.6	-81.9
Control of TNF	-81.4					
Control of AKT1		-88.6				
Control of EGFR			-67.0			
Control of MMP9				-109.5		
Control of PPARA					-90.8	
Control of HMGCR						-88.0

AKT1, MMP9, PPARA, and HMGCR. Meanwhile, bisdesmethoxycurcumin and myricetin were the most potent compounds against TNF and EGFR, respectively. The interaction profile of the best-scored compounds with their corresponding targets was illustrated in Fig. 5 and their percentage of similarity compared to the native ligands was presented in Table 7.

Table 5
Vina score of potential compounds against potential targets.

Compound	Vina score					
	TNF	AKT1	EGFR	MMP9	PPARA	HMGCR
β-sitosterol	–	-8.4	–	–	–	-5.9
Bisdesmethoxycurcumin	-9.4	-7.6	-7.8	–	-8.2	-6.5
Cucurbitacin D	–	-8.3	-8.7	–	–	-7.4
Cucurbitacin E	–	-9.0	–	–	–	-7.3
Myricetin	-8.4	-7.9	-8.9	-10.2	-6.7	-8.0
Phloretin	-8.6	–	-7.3	–	-6.8	-7.1
Quercitrin	–	–	-9.5	-8.5	-6.1	-8.4
Rutin	–	-8.7	-9.3	-8.4	-8.5	-8.9
Control of TNF	-13.0					
Control of AKT1		-8.5				
Control of EGFR			-7.3			
Control of MMP9				-10.9		
Control of PPARA					-12.0	
Control of HMGCR						-8.9

Table 6
Consensus score of potential compounds against potential targets.

Compound	Consensus score					
	TNF	AKT1	EGFR	MMP9	PPARA	HMGCR
β-sitosterol	–	-34.1	–	–	-	-30.6
Bisdesmethoxycurcumin	-37.1	-34.1	-32.4	–	-34.4	-29.4
Cucurbitacin D	–	-37.2	-33.7	-	-	-34.5
Cucurbitacin E	–	-38.3	–	-	-	-36.1
Myricetin	-30.5	-33.4	-33.9	-34.5	-29.3	-29.8
Phloretin	-29.6	–	-28.3	-	-27.7	-28.9
Quercitrin	–	–	-33.8	-36.7	-28.5	-36.7
Rutin	–	-48.8	-29.1	-43.4	-45.6	-45.4
Control of TNF	-47.2					
Control of AKT1		-48.6				
Control of EGFR			-37.2			
Control of MMP9				-60.2		
Control of PPARA					-51.4	
Control of HMGCR						-47.1

3.6. Inhibitory activity on HMGCR

The inhibitory activity of single extracts and their combination against HMGCR at 200 μg/mL was presented in Fig. 6. The extract combination showed the best inhibitory activity (85.91 %) followed by S. *polyanthum* (77.96 %), *C. xanthorrhiza* (73.44 %), and *S. edule* (54.78 %) extracts. The IC_{50} of the extract combination was shown in Fig. 7.

4. Discussion

In network pharmacology studies, topology parameters have been used as criteria for selecting potential compounds and targets. Compounds or targets with higher values of topology parameters indicate they play a significant role in the network. For this purpose, the mean values of every topology parameter have been used as the cutoff (Sun et al., 2021; Zhang et al., 2020). Based on PPI topology parameters and the degree of an active compound-target network, AKT1, EGFR, TNF, MMP9, PPARA, and HMGCR, were identified as the key targets for the antihyperlipidemic effect of this extract combination. Furthermore, KEGG analysis suggested that this extract combination might work by regulating multiple pathways. The most related pathways include insulin resistance, endocrine resistance, and AMPK signaling pathway.

Among the mentioned pathways, insulin resistance was the top pathway ranked by false discovery rate (FDR) ≤ 0.05. This pathway has been known to play an important role in the pathogenesis of hyperlipidemia through complex mechanisms (Bjornstad and Eckel, 2018; Howard, 1999). Meanwhile, endocrine resistance in several types of cancer such as prostate and breast cancer is associated with lipid metabolism (Hyder et al., 2021; Stoykova and Schlaepfer, 2019). One of the pathogenesis mechanisms of endocrine resistance involves the activation of the mevalonate pathway with HMGCR as the main enzyme to synthesize cholesterol (Hyder et al., 2021). Noteworthy, the mevalonate pathway is activated by the PI3K/AKT/mTORC1/SREBP pathway (Chimento et al., 2019; Porstmann et al., 2005). Hence, it's not surprising to find an accumulation of cholesterol in cancer cells (Kumar and Mandal, 2021), and several reports propose a promising role for statins in cancer treatment (Chimento et al., 2019). It might be the reason several cancer pathways were included in the top enriched pathways based on KEGG analysis. For AMPK signaling pathway, it plays a role in lipid homeostasis by regulating several downstream molecules, one of which is SREBP as discussed above. Phosphorylation of AMPK will inactivate SERBP (Li et al., 2011) along with its target, HMGCR.

In EGFR, a study using high-fat-diet-fed Mig-6d/d mice demonstrated that EGFR inhibition is effective for the treatment of hypercholesterolemia (Lee et al., 2014). EGFR has been known as one of the activators of PI3K/AKT/mTOR pathway. This study confirmed that after EGFR inhibitor (gefitinib) treatment, the phosphorylation level of AKT was reduced. MMP9 as well as TNF-α might be the target in hyperlipidemia treatment due to their role in atherosclerotic development (Prasad and Mishra, 2022; Tietge, 2014). Despite the mechanism not being clear yet, however, a study suggested that MMP9 acts as a pro-apoptotic and pro-inflammatory agent in endothelial cells via protease-activated receptor-1b (Tietge, 2014). Meanwhile, it has been shown that there is an improvement in lipid profiles and insulin resistance in patients with chronic inflammatory diseases by blocking TNF-α activity (Popa et al., 2007). PPARA has been recognized as a regulator of the metabolism of lipids, and its activators such as gemfibrozil and fenofibrate have been used in hypertriglyceridemia treatment

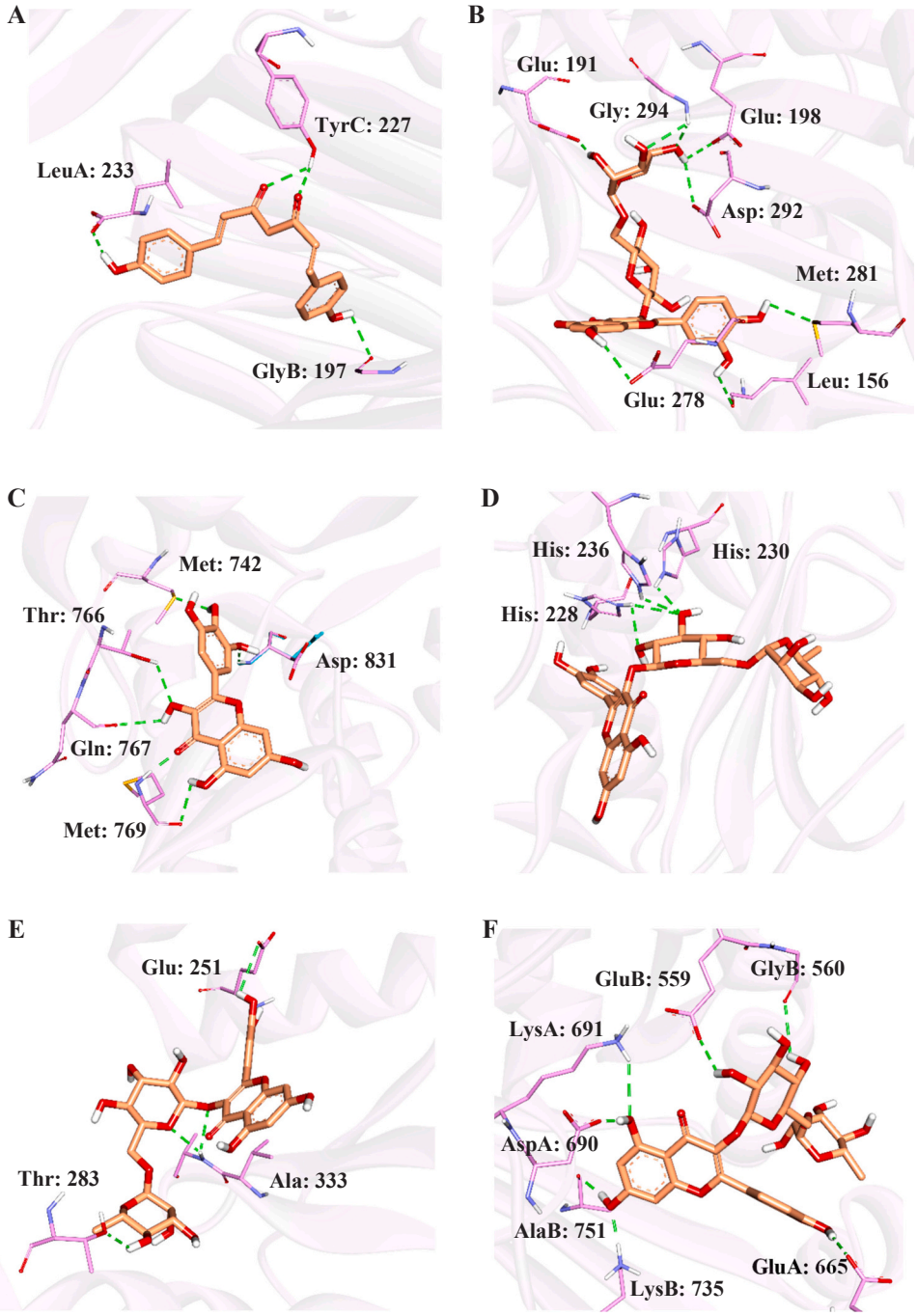

Fig. 5. Molecular docking of bisdesmethoxycurcumin on TNF (A); rutin on AKT1 (B); myricetin on EGFR (C); rutin on MMP9 (D); rutin on PPARA (E); rutin on HMGCR (F). Hydrogen bonds are shown in dashed green lines. Ligands are shown in orange sticks. Interacting residues of targets are shown in pink sticks.

(Monsalve et al., 2013; Villavicencio-Tejo et al., 2021).

A molecular docking study was conducted to verify that the proposed compounds can bind to the targets listed above. Recently, several docking tools have become available for docking simulation in the early steps of drug discovery. However, every tool may produce a different hit, or even if the hit is the same, its binding pose may be different in each tool. As shown in Tables 3 and 4, the ranking order of the compounds from DOCK6 and Vina was different. Therefore, we applied the consensus method by combining the results from the two docking tools. The consensus docking method was reported to reduce false positives (Gimeno et al., 2020). Compounds that showed duplet conformation in DOCK6 and Vina were considered true binders. Table 7 suggested that the best-scored compounds had similar interaction profiles to native ligands in the range of 38.5–75 %, indicating that they were in the binding pocket of the corresponding targets. They also were found to form hydrogen bonds with the key residues, similar to their native ligand.

Furthermore, HMGCR is an appealing target to be further investigated in regards to the mechanism of action of this extract combination due to its being the sole target in the docking study to produce duplet conformation for all compounds. The consensus score revealed that rutin was the compound with the best score in almost all targets. Rutin has been reported to reduce hypercholesterolemia through several mechanisms (Ziaee et al., 2009). Against HMGCR, rutin at a concentration of 10 μg/mL was reported to inhibit this enzyme activity by 60.17 % (Hartanti et al., 2019). According to our docking simulation, this

Table 7
Interaction profile of the best-scored compounds and native ligands on their corresponding target.

Target	Amino acid residues		Similarity
	Best-scored compound	Native ligand	
TNF	LeuA133, LeuC133, TyrA135, GlyB197*, TyrC227*, LeuA233*	LeuA133, LeuC133, TyrA135, TyrC135,TyrB195*, TyrC195, TyrC227*, LeuA233*	62.5 %
AKT1	Leu156*, Gly159, Leu181, Glu191*, Glu198*, Glu234, Glu278*, Met281*, Asp292*, Gly294*	Leu156, Gly157, Gly162, Val164, Ala177, Lys179, Leu181, Met227, Ala230*, Glu234*, Glu278*, Asn279, Met281*	38.5 %
EGFR	Leu694, Val702, Ala719, Lys721, Met742*, Thr766*, Gln767*, Met769*, Leu820, Asp831*	Leu694, Ala719, Lys721, Leu764, Gln767, Met769*, Leu820, Thr830	75 %
MMP9	Tyr179, Leu188, Ala189, His190, Val223, His226*, His230*, His236*, Met247	Leu188*, Ala189*, Ala191*, His226, His230, His236, Pro246, Glu277	62.5 %
PPARA	Ile241, Ala250, Glu251*, Val255, Cys275, Cys276, Thr283*, Met330, Val332, Ala333*, Tyr334, Ile339	Val255, Phe273, Cys275, Cys276, Thr279*, Tyr314*, Met330, Val332, Ile339, Leu344, Met355, His440, Val444, Tyr464*	46.2 %
HMGCR	GluB559*, GlyB560*, ArgA590, AsnA658, GluA665*, ValA683, AspA690*, LysA691*, LysB735*, AlaB751*, LeuB853, AlaB856	GluB559*, CysB561, LeuB562, AlaB564, SerB565*, ArgA590*, SerA661*, ValA683, SerA684*, AspA690*, LysA691*, LysB735*, HisB752, AsnB755*, LeuB853, AlaB856	50 %

*Residues formed H-bond with the ligands. The green text indicates the same residues that interact with the best-scored compounds and the native ligands. The percentage of similarity represents the number of the same residues (green text) in the best-scored compound of the total residues that interact with the native ligand.

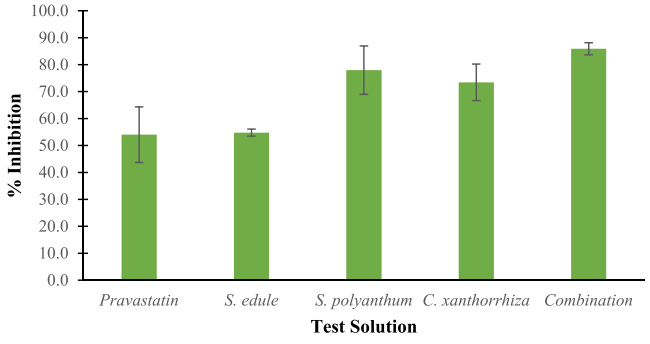

Fig. 6. Percentage of inhibition of pravastatin (0.02 μg/mL), and extracts (200 μg/mL) against HMGCR.

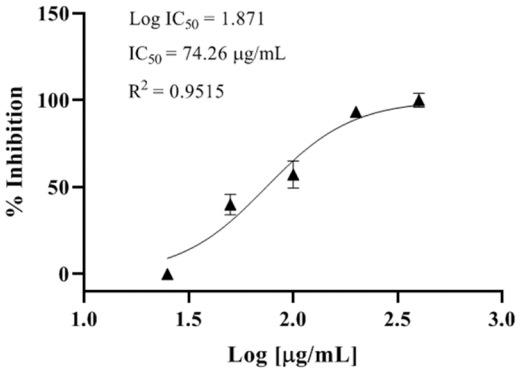

Fig. 7. Dose-response curve of extract combination.

compound was found to be inserted into the HMGCR dimer and form hydrogen bonds with GluB559, GlyB560, GluA665, AspA690, LysA691, LysB735, and AlaB751.

A study demonstrated that rutin has a protective effect on spinal cord injury by inhibiting MMP9 activation and reducing AKT1 expression (Zhang and Ma, 2015). Our docking simulation revealed that rutin formed hydrogen bonds with AKT1 at Leu156, Glu191, Glu198, Glu278, Met281, Asp292, and Gly294. On MMP9, it formed hydrogen bonds with His226, His230, and His236.

Docking research on PPARA indicated that rutin has a better binding affinity compared to orlistat. This has been confirmed experimentally using adipocyte culture where rutin showed better lipid inhibition than orlistat (Mandal et al., 2022). A kinase assay experiment also revealed that rutin can suppress EGFR activity directly (Choi et al., 2013). Myricetin, the best-scored compound on EGFR in our docking study (Table 6), could decrease phosphorylated EGFR levels based on a western blot assay (Li et al., 2020). We found that it formed hydrogen bonds with Met742, Thr766, Gln767, Met769, and Asp831. Bisdesmethoxycurcumin was reported to have inflammatory activity by down-regulating TNF α-induced NF-kappa B and was stronger than curcumin (Jain, 2020). This compound formed hydrogen bonds with GlyB197, TyrC227, and LeuA233 on TNF.

Furthermore, at the extract level, a study demonstrated that an ethanol extract from *S. polyanthum* leaf inhibited 65.71 % of HMGCR activity at 150 μg/mL (Hartanti et al., 2019). In our study, this extract inhibited 78.0 % of HMGCR activity at 200 μg/mL. Overall, based on the single concentration test, each extract and its combination were verified

to inhibit the activity of HMGCR. Several studies have reported their extract potency in inhibiting HMGCR activity with an IC_{50} in the range of 9.1–452.6 μg/mL (Ademosun et al., 2015; Grande et al., 2021; Iqbal et al., 2014). In the present study, the extract combination showed inhibitory activity with an IC_{50} value of 74.26 μg/mL, indicating that HMGCR inhibition is one of its antihyperlipidemic mechanisms.

Other experimental studies also showed that ethanol extracts of *S. edule* fruit and *C. xanthorriza* rhizome work as anti-insulin resistance agents (Kim et al., 2014; Villavicencio-Tejo et al., 2021), which is the most significant pathway based on KEGG analysis. The above-mentioned reports support our network pharmacology and molecular docking predictions in explaining the mechanism of action of this extract combination.

5. Conclusion

In the current study, we combined network pharmacology and molecular docking studies to explore the potential compounds of the combined extracts of *C. xanthorrhiza* Rhizome, *S. edule* Fruit, and *S. polyanthum* Leaf and their potential targets. The network pharmacology results suggested there were 8 potential compounds: β-sitosterol, bisdesmethoxycurcumin, cucurbitacin D, cucurbitacin E, myricetin, phloretin, quercitrin, and rutin, which work multitargeted, especially against HMGCR, PPARA, AKT1, EGFR, MMP9, and TNF as the potential targets. Furthermore, docking simulations with the consensus method revealed that HMGCR is an attractive target because it can be targeted by all potential compounds. The in vitro study confirmed that the extract combination could work on HMGCR with $IC_{50} = 74.26$ μg/mL. However, the remaining potential targets still need to be validated experimentally. We predicted that the extract combination works as an antihyperlipidemic by regulating multiple pathways, including insulin resistance, endocrine resistance, and the AMPK signaling pathway.

Funding

This research did not receive any specific grant from funding agencies in the public, commercial, or not-for-profit sectors.

CRediT authorship contribution statement

Frangky Sangande performed the computational and in vitro experiments, analyzed the data, and drafted the manuscript; Kurnia Agustini designed the methodology, analyzed the data, and corrected the manuscript; Krisyanti Budipramana analyzed the data and corrected the manuscript. All authors have read and agreed to the published version of the manuscript.

Declaration of Competing Interest

The authors declare that they have no known competing financial interests or personal relationships that could have appeared to influence the work reported in this paper.

References

Ademosun, A.O., Oboh, G., Passamonti, S., Tramer, F., Ziberna, L., Augusti Boligon, A., Linde Athayde, M., 2015. Phenolics from grapefruit peels inhibit HMG-CoA reductase and angiotensin-I converting enzyme and show antioxidative properties in endothelial EA.Hy 926 cells. Food Sci. Hum. Wellness 4, 80–85. https://doi.org/10.1016/j.fshw.2015.05.002.

Agustini, K., Azizahwati, A., Marlina, S., 2006. Duration effect of administration formula containing *Sechium edule* fruit extract on decreasing total cholesterol and triglyceride levels in male albino rats. J. Bahan Alam Indones. 6, 60–62.

Arifah, F.H., Nugroho, A.E., Rohman, A., Sujarwo, W., 2022. A review of medicinal plants for the treatment of diabetes mellitus: the case of Indonesia. S. Afr. J. Bot. 149, 537–558. https://doi.org/10.1016/j.sajb.2022.06.042.

Atanasov, A.G., Zotchev, S.B., Dirsch, V.M., Orhan, I.E., Banach, M., Rollinger, J.M., Barreca, D., Weckwerth, W., Bauer, R., Bayer, E.A., Majeed, M., Bishayee, A., Bochkov, V., Bonn, G.K., Braidy, N., Bucar, F., Cifuentes, A., D'Onofrio, G., Bodkin, M., Diederich, M., Dinkova-Kostova, A.T., Efferth, T., El Bairi, K., Arkells, N., Fan, T.P., Fiebich, B.L., Freissmuth, M., Georgiev, M.I., Gibbons, S., Godfrey, K.M., Gruber, C.W., Heer, J., Huber, L.A., Ibanez, E., Kijjoa, A., Kiss, A.K., Lu, A., Macias, F. A., Miller, M.J.S., Mocan, A., Müller, R., Nicoletti, F., Perry, G., Pittalà, V., Rastrelli, L., Ristow, M., Russo, G.L., Silva, A.S., Schuster, D., Sheridan, H., Skalicka-Woźniak, K., Skaltsounis, L., Sobarzo-Sánchez, E., Bredt, D.S., Stuppner, H., Sureda, A., Tzvetkov, N.T., Vacca, R.A., Aggarwal, B.B., Battino, M., Giampieri, F., Wink, M., Wolfender, J.L., Xiao, J., Yeung, A.W.K., Lizard, G., Popp, M.A., Heinrich, M., Berindan-Neagoe, I., Stadler, M., Daglia, M., Verpoorte, R., Supuran, C. T., 2021. Natural products in drug discovery: advances and opportunities. Nat. Rev. Drug Discov. 20, 200–216. https://doi.org/10.1038/s41573-020-00114-z.

Bjornstad, P., Eckel, R.H., 2018. Pathogenesis of lipid disorders in insulin resistance: a brief review. Curr. Diab. Rep. 18, 1–8. https://doi.org/10.1007/S11892-018-1101-6.

Che, C.T., Wang, Z.J., Chow, M.S.S., Lam, C.W.K., 2013. Herb-herb combination for therapeutic enhancement and advancement: Theory, practice and future perspectives. Molecules 18, 5125–5141. https://doi.org/10.3390/molecules18055125.

Chimento, A., Casaburi, I., Avena, P., Trotta, F., De Luca, A., Rago, V., Pezzi, V., Sirianni, R., 2019. Cholesterol and its metabolites in tumor growth: therapeutic potential of statins in cancer treatment. Front. Endocrinol. 9, 807. https://doi.org/10.3389/fendo.2018.00807.

Choi, S., Lim, T.G., Hwang, M.K., Kim, Y.A., Kim, J., Kang, N.J., Jang, T.S., Park, J.S., Yeom, M.H., Lee, K.W., 2013. Rutin inhibits B[a]PDE-induced cyclooxygenase-2 expression by targeting EGFR kinase activity. Biochem. Pharmacol. 86, 1468–1475. https://doi.org/10.1016/j.bcp.2013.08.066.

Gimeno, A., Mestres-Truyol, J., Ojeda-Montes, M.J., Macip, G., Saldivar-Espinoza, B., Cereto-Massagué, A., Pujadas, G., Garcia-Vallvé, S., 2020. Prediction of novel inhibitors of the main protease (M-pro) of SARS-CoV-2 through consensus docking and drug reposition. Int. J. Mol. Sci. 21, 3793. https://doi.org/10.3390/ijms21113793.

Grande, F., Occhiuzzi, M.A., Perri, M.R., Ioele, G., Rizzuti, B., Statti, G., Garofalo, A., 2021. Polyphenols from Citrus Tacle® extract endowed with HMGCR inhibitory activity: an antihypercholesterolemia natural remedy. Molecules 26, 5718. https://doi.org/10.3390/molecules26185718.

Hartanti, L., Yonas, S.M.K., Mustamu, J.J., Wijaya, S., Setiawan, H.K., Soegianto, L., 2019. Influence of extraction methods of bay leaves (*Syzygium polyanthum*) on antioxidant and HMG-CoA Reductase inhibitory activity. Heliyon 5, e01485. https://doi.org/10.1016/j.heliyon.2019.E01485.

Hasani-Ranjbar, S., Nayebi, N., Moradi, L., Mehri, A., Larijani, B., Abdollahi, M., 2012. The efficacy and safety of herbal medicines used in the treatment of hyperlipidemia; a systematic review. Curr. Pharm. Des. 16, 2935–2947. https://doi.org/10.2174/138161210793176464.

Howard, B.V., 1999. Insulin resistance and lipid metabolism. Am. J. Cardiol. 84, 28–32. https://doi.org/10.1016/s0002-9149(99)00355-0.

Hyder, T., Marti, J.L.G., Nasrazadani, A., Brufsky, A.M., 2021. Statins and endocrine resistance in breast cancer. Cancer Drug Resist. 4, 356–364. https://doi.org/10.20517/cdr.2020.112.

Iñiguez-Luna, M.I., Cadena-Iñiguez, J., Soto-Hernández, R.M., Morales-Flores, F.J., Cortes-Cruz, M., Watanabe, K.N., 2021. Natural bioactive compounds of *Sechium* spp. for therapeutic and nutraceutical supplements. Front. Plant Sci. 12, 772389 https://doi.org/10.3389/fpls.2021.772389.

Iqbal, D., Khan, Mohd, Salman, Khan, A., Khan, Mohd, Sajid, Ahmad, S., Srivastava, A.K., Bagga, P., 2014. In vitro screening for β-hydroxy-β-methylglutaryl-CoA reductase inhibitory and antioxidant activity of sequentially extracted fractions of *Ficus palmata* forsk. Biomed. Res. Int. 2014, 762620 https://doi.org/10.1155/2014/762620.

Ismail, A., Ahmad, W., Ahmad, W., Ahmad, W., 2019. Syzygium polyanthum (Wight) walp: A potential phytomedicine. Pharmacogn. J. 11, 429–438. https://doi.org/10.5530/pj.2019.11.67.

Jain, R., 2020. Biological activities of bisdesmethoxycurcumin. J. Nat. Sci. Med. 3, 219–220. https://doi.org/10.4103/jnsm.jnsm_65_19.

Kim, M.-B., Kim, C., Song, Y., Hwang, J.-K., 2014. Antihyperglycemic and antiinflammatory effects of standardized *Curcuma xanthorrhiza* Roxb. extract and its active compound xanthorrhizol in high-fat diet-induced obese mice. Evid. Based Complement. Altern. Med. 2014, 205915 https://doi.org/10.1155/2014/205915.

Kumar, N., Mandal, C.C., 2021. Cholesterol-lowering drugs on Akt signaling for prevention of tumorigenesis. Front. Genet. 12, 1706. https://doi.org/10.3389/fgene.2021.724149.

Lau, K.M., Lai, K.K., Liu, C.L., Tam, J.C.W., To, M.H., Kwok, H.F., Lau, C.P., Ko, C.H., Leung, P.C., Fung, K.P., Poon, S.K.S., Lau, C.B.S., 2012. Synergistic interaction between Astragali Radix and Rehmanniae Radix in a Chinese herbal formula to promote diabetic wound healing. J. Ethnopharmacol. 141, 250–256. https://doi.org/10.1016/j.jep.2012.02.025.

Lee, J.C., Park, B.K., Choung, S., Kim, J.M., Joung, K.H., Lee, J.H., Kim, K.S., Kim, H.J., Jeong, J.W., Rhee, S.D., Ku, B.J., 2014. Amelioration of hypercholesterolemia by an EGFR tyrosine kinase inhibitor in mice with liver-specific knockout of mig-6. PLoS One 9, e114782. https://doi.org/10.1371/journal.pone.0114782.

Li, W., Xu, C., Hao, C., Zhang, Y., Wang, Z., Wang, S., Wang, W., 2020. Inhibition of herpes simplex virus by myricetin through targeting viral gD protein and cellular EGFR/PI3K/Akt pathway. Antivir. Res. 177, 104714 https://doi.org/10.1016/j.antiviral.2020.104714.

Li, X., Wei, S., Niu, S., Ma, X., Li, H., Jing, M., Zhao, Y., 2022. Network pharmacology prediction and molecular docking-based strategy to explore the potential mechanism of Huanglian Jiedu Decoction against sepsis. Comput. Biol. Med. 144, 105389 https://doi.org/10.1016/j.compbiomed.2022.105389.

Li, Y., Xu, S., Mihaylova, M.M., Zheng, B., Hou, X., Jiang, B., Park, O., Luo, Z., Lefai, E., Shyy, J.Y.J., Gao, B., Wierzbicki, M., Verbeuren, T.J., Shaw, R.J., Cohen, R.A., Zang, M., 2011. AMPK phosphorylates and inhibits SREBP activity to attenuate hepatic steatosis and atherosclerosis in diet-induced insulin-resistant mice. Cell Metab. 13, 376–388. https://doi.org/10.1016/j.cmet.2011.03.009.

Liu, J., Yuan, S., Yao, Y., Wang, J., Scalabrino, G., Jiang, S., Sheridan, H., 2022. Network pharmacology and molecular docking elucidate the underlying pharmacological mechanisms of the herb *Houttuynia cordata* in treating pneumonia caused by SARS-CoV-2. Viruses 14, 1588. https://doi.org/10.3390/v14071588.

Mandal, S.K., Kumar, B.K., Sharma, P.K., Murugesan, S., Deepa, P.R., 2022. In silico and in vitro analysis of PPAR–α/γ dual agonists: comparative evaluation of potential phytochemicals with anti-obesity drug orlistat. Comput. Biol. Med. 147, 105796 https://doi.org/10.1016/j.compbiomed.2022.105796.

Mohammed, F.S., Ghosh, A., Pal, S., Das, C., Alomar, S.Y., Patwekar, M., Patwekar, F., Jeon, B.H., Islam, F., 2022. Hydroalcoholic extract of *Sechium edule* fruits attenuates QT prolongation in high fat diet-induced hyperlipidemic mice. Evidence-based Complement. Altern. Med. 2022, 8682316. https://doi.org/10.1155/2022/8682316.

Monsalve, F.A., Pyarasani, R.D., Delgado-Lopez, F., Moore-Carrasco, R., 2013. Peroxisome proliferator-activated receptor targets for the treatment of metabolic diseases. Mediat. Inflamm. 2013, 549627 https://doi.org/10.1155/2013/549627.

Nelson, R.H., 2013. Hyperlipidemia as a risk factor for cardiovascular disease. Prim. Care 40, 195–211. https://doi.org/10.1016/j.pop.2012.11.003.

Noor, F., Qamar, M.T.U., Ashfaq, U.A., Albutti, A., Alwashmi, A.S.S., Aljasir, M.A., 2022. Network pharmacology approach for medicinal plants: review and assessment. Pharmaceuticals 15, 572. https://doi.org/10.3390/ph15050572.

Ou-Yang, S.S., Lu, J.Y., Kong, X.Q., Liang, Z.J., Luo, C., Jiang, H., 2012. Computational drug discovery. Acta Pharmacol. Sin. 33, 1131–1140. https://doi.org/10.1038/aps.2012.109.

Popa, C., Netea, M.G., Van Riel, P.L.C.M., Van Der Meer, J.W.M., Stalenhoef, A.F.H., 2007. The role of TNF-alpha in chronic inflammatory conditions, intermediary metabolism, and cardiovascular risk. J. Lipid Res. 48, 751–752. https://doi.org/10.1194/jlr.r600021-jlr200.

Porstmann, T., Griffiths, B., Chung, Y.L., Delpuech, O., Griffiths, J.R., Downward, J., Schulze, A., 2005. PKB/Akt induces transcription of enzymes involved in cholesterol and fatty acid biosynthesis via activation of SREBP. Oncogene 24, 6465–6481. https://doi.org/10.1038/sj.onc.1208802.

Prasad, K., Mishra, M., 2022. Mechanism of hypercholesterolemia-induced atherosclerosis. Rev. Cardiovasc. Med. 23, 212. https://doi.org/10.31083/j.rcm2306212.

Riviello-Flores, M., de la, L., Arévalo-Galarza, M., de, L., Cadena-Iñiguez, J., Soto-Hernández, R.M., Ruiz-Posadas, L.D.M., Gómez-Merino, F.C., 2018. Nutraceutic characteristics of the extracts and juice of chayote (*Sechium edule* (Jacq.) Sw.) fruits. Beverages 4, 37. https://doi.org/10.3390/beverages4020037.

Stoykova, G.E., Schlaepfer, I.R., 2019. Lipid metabolism and endocrine resistance in prostate cancer, and new opportunities for therapy. Int. J. Mol. Sci. 20, 2626. https://doi.org/10.3390/ijms20112626.

Su, L., Mittal, R., Ramgobin, D., Jain, Rahul, Jain, Rohit, 2021. Current management guidelines on hyperlipidemia: the silent killer. J. Lipids 2021, 1–5. https://doi.org/10.1155/2021/9883352.

Sun, R., Xu, G., Gao, D., Ding, Q., Shi, Y., 2021. To predict anti-inflammatory and immunomodulatory targets of guizhi decoction in treating asthma based on network pharmacology, molecular docking, and experimental validation. Evid. Based Complement. Altern. Med. 2021, 9033842. https://doi.org/10.1155/2021/9033842.

Sun, Y., Feng, F., Yu, X., 2012. Pharmacokinetics of geniposide in Zhi-Zi-Hou-Pu decoction and in different combinations of its constituent herbs. Phyther. Res. 26, 67–72. https://doi.org/10.1002/ptr.3516.

Tietge, U.J.F., 2014. Hyperlipidemia and cardiovascular disease: Inflammation, dyslipidemia, and atherosclerosis. Curr. Opin. Lipidol. 25, 94–95. https://doi.org/10.1097/mol.0000000000000051.

Villavicencio-Tejo, F., Flores-Bastías, O., Marambio-Ruiz, L., Pérez-Reytor, D., Karahanian, E., 2021. Fenofibrate (a PPAR-α agonist) administered during ethanol withdrawal reverts ethanol-induced astrogliosis and restores the levels of glutamate transporter in ethanol-administered adolescent rats. Front. Pharmacol. 12, 653175 https://doi.org/10.3389/fphar.2021.653175.

Wu, H., Shu, W., Qiu, L., Ye, D., 1998. The experiment research of ginger detoxification to rhizoma Pinelliae. Zhong Yao Cai 21, 137–140.

Yasni, S., Imaizumi, K., Nakamura, M., Aimoto, J., Sugano, M., 1993. Effects of *Curcuma xanthorrhiza* Roxb. and curcuminoids on the level of serum and liver lipids, serum apolipoprotein A-I and lipogenic enzymes in rats. Food Chem. Toxicol. 31, 213–218. https://doi.org/10.1016/0278-6915(93)90096-h.

Zhang, Laigen, Shi, X., Huang, Z., Mao, J., Mei, W., Ding, L., Zhang, Li, Xing, R., Wang, P., 2020. Network pharmacology approach to uncover the mechanism governing the effect of radix achyranthis bidentatae on osteoarthritis. BMC Complement. Med. Ther. 20, 121. https://doi.org/10.1186/s12906-020-02909-4.

Zhang, M., Yang, J., Zhao, X., Zhao, Y., Zhu, S., 2021. Network pharmacology and molecular docking study on the active ingredients of qidengmingmu capsule for the treatment of diabetic retinopathy. Sci. Rep. 11, 1–11. https://doi.org/10.1038/s41598-021-86914-8.

Zhang, P., Ma, X., 2015. Effect of rutin on spinal cord injury through inhibition of the expression of MIP-2 and activation of MMP-9, and downregulation of Akt phosphorylation. Mol. Med. Rep. 12, 7554–7560. https://doi.org/10.3892/mmr.2015.4357.

Zhou, X., Seto, S.W., Chang, D., Kiat, H., Razmovski-Naumovski, V., Chan, K., Bensoussan, A., 2016. Synergistic effects of Chinese herbal medicine: a comprehensive review of methodology and current research. Front. Pharmacol. 7, 201. https://doi.org/10.3389/fphar.2016.00201.

Ziaee, A., Zamansoltani, F., Nassiri-Asl, M., Abbasi, E., 2009. Effects of rutin on lipid profile in hypercholesterolaemic rats. Basic Clin. Pharmacol. Toxicol. 104, 253–258. https://doi.org/10.1111/j.1742-7843.2008.00368.x.

Volume 195, October 2003 ISSN 1476-9271

Computational Biology and Chemistry

Editors: Wenbian Li, Donald Hamelberg

www.elsevier.com/locate/cbac

Computational Biology and Chemistry

Computational Biology and Chemistry

Supports *open access*

6.4 CiteScore

3.1 Impact Factor

Volume 105

August 2023

Research article Full text access

Inflammation inhibitory activity of green tea, soybean, and guava extracts during Sars-Cov-2 infection through TNF protein in cytokine storm

Didik Priyandoko, Wahyu Widowati, Hanna Sari Widya Kusuma, Ervi Afifah, ... Didik Huswo Utomo
Article 107898

View PDF Article preview

Research article Full text access

Integrated transcriptomics and proteomics data analysis identifies CDH17 as a key cell surface target in colorectal cancer

Kah Keng Wong
Article 107897

View PDF Article preview

Research article Full text access

Design, synthesis, molecular dynamics simulation, MM/GBSA studies and kinesin spindle protein inhibitory evaluation of some 4-aminoquinoline hybrids

Shriram D. Ranade, Shankar G. Alegaon, U. Venkatasubramanian, A. Soundarya Priya, ... D. Vinod
Article 107881

View PDF Article preview

Research article Full text access

CTDN (Convolutional Temporal Based Deep- Neural Network): An Improvised Stacked Hybrid Computational Approach for Anticancer Drug Response Prediction

Davinder Paul Singh, Baijnath Kaushik
Article 107868

View PDF Article preview

Research article Full text access

HR-LCMS and evaluation of anti-diabetic activity of *Hemidesmus indicus* (anantmool): Kinetic study, and molecular modelling approach

Sonali Kumari, Ravi Saini, Aditi Bhatnagar, Abha Mishra
Article 107896

View PDF Article preview

Research article *Open access*

Graph-ETMB: A graph neural network-based model for tumour mutation burden estimation

Wanting Yang, Yan Qiang, Wei Wu, Jialong Xin
Article 107900

View PDF Article preview

Research article Full text access

Halogenated class of oximes as a new class of monoamine oxidase-B inhibitors for the treatment of Parkinson's disease: Synthesis, biochemistry, and molecular dynamics study

Della Grace Thomas Parambi, Jong Min Oh, Sunil Kumar, Sachithra Thazhathuveedu Sudevan, ... Bijo Mathew
Article 107899

View PDF Article preview

Research article Full text access

Lycopene destabilizes preformed Aβ fibrils: Mechanistic insights from all-atom molecular dynamics simulation

Shivani Gupta, Ashok Kumar Dasmahapatra
Article 107903

View PDF Article preview

Research article *Open access*

TSSUNet-MB – *ab initio* identification of σ^{70} promoter transcription start sites in *Escherichia coli* using deep multitask learning

Chung-En Ni, Duy-Phuong Doan, Yen-Jung Chiu, Yen-Hua Huang
Article 107904

View PDF Article preview

Research article *Open access*

A convolutional network and attention mechanism-based approach to predict protein–RNA binding residues

Ke Li, Hongwei Wu, Zhenyu Yue, Yu Sun, Chuan Xia
Article 107901

View PDF Article preview

Research article Full text access

MMDAE-HGSOC: A novel method for high-grade serous ovarian cancer molecular subtypes classification based on multi-modal deep autoencoder

Hui-Qing Wang, Hao-Lin Li, Jia-Le Han, Zhi-Peng Feng, ... Xiao Han
Article 107906

View PDF Article preview

Research article Full text access

SENet: A deep learning framework for discriminating super- and typical enhancers by sequence information

Hanyu Luo, Ye Li, Huan Liu, Pingjian Ding, ... Lingyun Luo
Article 107905

View PDF Article preview

Research article Full text access

Drug repurposing for Basal breast cancer subpopulations using modular network signatures

Hiram Coria-Rodríguez, Soledad Ochoa, Guillermo de Anda-Jáuregui, Enrique Hernández-Lemus
Article 107902

View PDF Article preview

Research article Full text access

Designing, characterization, biological, DFT, and molecular docking analysis for new FeAZD, NiAZD, and CuAZD complexes incorporating 1-(2-hydroxyphenylazo)−2-naphthol (H_2AZD)

Hany M. Abd El-Lateef, Mai M. Khalaf, Mahmoud Kandeel, Amer A. Amer, ... Aly Abdou
Article 107908

View PDF Article preview

Research article Full text access

Antihyperlipidemic mechanisms of a formula containing *Curcuma xanthorrhiza, Sechium edule,* and *Syzigium polyanthum*: In silico and in vitro studies

Frangky Sangande, Kurnia Agustini, Krisyanti Budipramana
Article 107907

View PDF Article preview

Research article Full text access

Halting aberrant DNA methylation via *in silico* Identification of potent inhibitors of DNMT3B enzyme: Atomistic insights

Lusanda M. Mtetwa, Elliasu Y. Salifu, Calvin A. Omolo, Mahmoud E. Soliman, Mbuso. Faya
Article 107909

View PDF Article preview

Previous vol/issue Next vol/issue

ISSN: 1476-9271

Computational Biology and Chemistry

COUNTRY

United Kingdom

Universities and research institutions in United Kingdom

Media Ranking in United Kingdom

SUBJECT AREA AND CATEGORY

Biochemistry, Genetics and Molecular Biology
- Biochemistry
- Structural Biology

Chemistry
- Organic Chemistry

Mathematics
- Computational Mathematics

PUBLISHER

Elsevier Ltd.

H-INDEX

65

PUBLICATION TYPE

Journals

ISSN

14769271

COVERAGE

2003-2022

INFORMATION

Homepage

How to publish in this journal

Contact

SCOPE

Computational Biology and Chemistry publishes original research papers and review articles in all areas of computational life sciences. High quality research contributions with a major computational component in the areas of nucleic acid and protein sequence research, molecular evolution, molecular genetics (functional genomics and proteomics), theory and practice of either biology-specific or chemical-biology-specific modeling, and structural biology of nucleic acids and proteins are particularly welcome. Exceptionally high quality research work in bioinformatics, systems biology, ecology, computational pharmacology, metabolism, biomedical engineering, epidemiology, and statistical genetics will also be considered. Given their inherent uncertainty, protein modeling and molecular docking studies should be thoroughly validated. In the absence of experimental results for validation, the use of molecular dynamics simulations along with detailed free energy calculations, for example, should be used as complementary techniques to support the major conclusions. Submissions of premature modeling exercises without additional biological insights will not be considered. Review articles will generally be commissioned by the editors and should not be submitted to the journal without explicit invitation. However prospective authors are welcome to send a brief (one to three pages) synopsis, which will be evaluated by the editors.

Quartiles

FIND SIMILAR JOURNALS

options

1
Interdisciplinary Sciences - Computational Life Sciences
DEU

2
International Journal of Computational Biology and
GBR

3
Computational and Structural Biotechnology Journal
SWE

4
International Journal of Bioinformatics Research and
GBR

5
Bioinformatics and Biology Insights
NZL

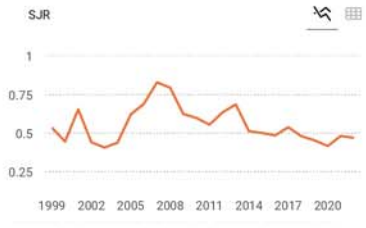

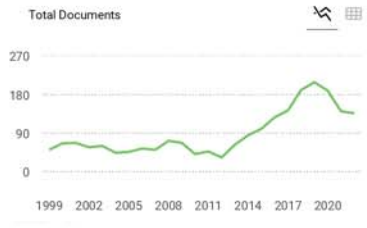

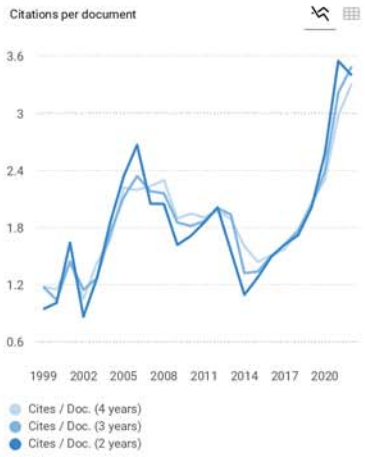

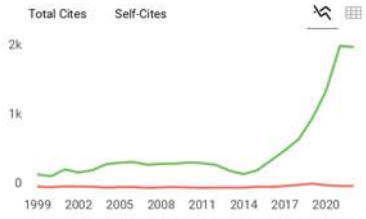

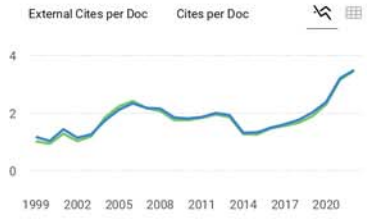

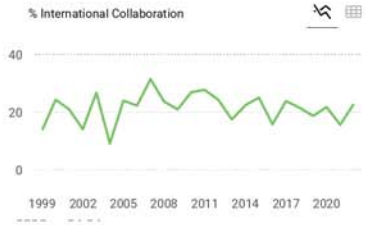

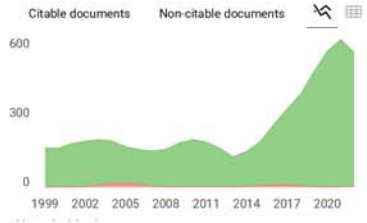

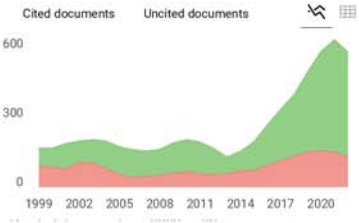

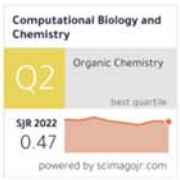

← Show this widget in your own website

Just copy the code below and paste within your html code:

<a href="https://www.scim

SCImago Graphica

Explore, visually communicate and make sense of data with our **new data visualization tool**.

Metrics based on Scopus® data as of April 2023

R **Ramesh** 2 years ago

Can Computational Biology and Chemistry journal publish the all the field about computational chemistry?

reply

SCImago Team

Melanie Ortiz 2 years ago

Dear Ramesh,
Thank you for contacting us.
We suggest you visit the journal's homepage or contact the journal's editorial staff , so they could inform you more deeply.
Best Regards, SCImago Team

Leave a comment

Name

Email
(will not be published)

Submit

The users of Scimago Journal & Country Rank have the possibility to dialogue through comments linked to a specific journal. The purpose is to have a forum in which general doubts about the processes of publication in the journal, experiences and other issues derived from the publication of papers are resolved. For topics on particular articles, maintain the dialogue through the usual channels with your editor.

Source details

Computational Biology and Chemistry

Formerly known as: Computers and Chemistry

Scopus coverage years: from 2003 to Present

Publisher: Elsevier

ISSN: 1476-9271

Subject area: Mathematics: Computational Mathematics | Chemistry: Organic Chemistry | Biochemistry, Genetics and Molecular Biology: Structural Biology | Biochemistry, Genetics and Molecular Biology: Biochemistry

Source type: Journal

CiteScore 2022
6.4

SJR 2022
0.469

SNIP 2022
0.822

View all documents > | Set document alert | Save to source list | Source Homepage

CiteScore | CiteScore rank & trend | Scopus content coverage

CiteScore 2022

$$6.4 = \frac{4{,}257 \text{ Citations } 2019 - 2022}{668 \text{ Documents } 2019 - 2022}$$

Calculated on 05 May, 2023

CiteScoreTracker 2023

$$5.2 = \frac{2{,}969 \text{ Citations to date}}{569 \text{ Documents to date}}$$

Last updated on 05 September, 2023 • Updated monthly

CiteScore rank 2022

Category	Rank	Percentile
Mathematics └ Computational Mathematics	#16/172	90th
Chemistry └ Organic Chemistry	#54/197	72nd
Biochemistry, Genetics and Molecular Biology	#18/45	61st

View CiteScore methodology > | CiteScore FAQ > | Add CiteScore to your site

About Scopus

What is Scopus

Content coverage

Scopus blog

Scopus API

Privacy matters

Language

日本語版を表示する

查看简体中文版本

查看繁體中文版本

Просмотр версии на русском языке

Customer Service

Help

Tutorials

Contact us